Structural Origin of Dynamical Heterogeneity in a Binary Lennard-Jones Liquid

M. Shajahan G. Razul, Gurpreet S. Matharoo, and Peter H. Poole
Department of Physics, St. Francis Xavier University, Antigonish, NS, B2G 2W5, Canada
(Dated: February 18, 2009)

We use isoconfigurational ensemble simulations to analyze dynamical heterogeneity (DH) and structural heterogeneity (SH) as a function of temperature T in the supercooled Kob-Andersen binary Lennard-Jones liquid. At high T we identify SH that is larger than the observed DH. As T decreases, the DH grows but remains smaller than or comparable in size to the SH at all T studied. Our results thus elucidate the structural origin of DH in this important model glass-former.

PACS numbers: 64.70.Pf,05.60.Cd,61.43.Fs,81.05.Kf

arXiv:0902.3255v1 [cond-mat.mtrl-sci] 18 Feb 2009

Glass-forming liquids are remarkable for the extraordinary sensitivity of their transport properties to changes in state variables, such as temperature T [1]. Properties such as viscosity are commonly found to vary over 14 orders of magnitude in supercooled liquids between the melting temperature and the glass transition. Yet in the same interval of T, it is also typical that only modest changes occur in the average liquid structure. One of the central questions in the study of the glass transition is whether this enormous dynamical response can be understood in terms of structural change [2].

Much recent interest has focussed on the emergence and growth of dynamical heterogeneity (DH) in supercooled liquids, that is, spatially extended domains in which molecules are more or less mobile, relative to the bulk average [3]. The growth of these dynamical domains as T decreases seems to occur in the absence of a growing structural length scale. At the same time, the simulation work of Widmer-Cooper, Harrowell and coworkers has shown that key aspects of DH are indeed structural in origin [4, 5, 6]. They do so through the use of the "isoconfigurational (IC) ensemble", a simulation procedure in which a given liquid configuration is analyzed by conducting a set of runs all initiated from the same configuration, but in which particle velocities are randomized [4]. Analysis of the"dynamic propensity", a particle's displacement averaged over all the runs of the IC ensemble, reveals spatial heterogeneity that can only be due to structural properties of the initial configuration, since the effect of the velocity initial conditions has been averaged out.

In this Letter, we evaluate the dynamic propensity in the Kob-Andersen binary Lennard-Jones liquid [7], a model system that has received much attention in simulations of glass-forming liquids in general [8], and in the analysis of DH in particular [9, 10, 11, 12]. We also analyze the structure of the liquid via IC averaging, and show that structural heterogeneity (SH) exists at high T that is greater in size than the DH occurring at the same T. Further, as T decreases and the DH grows, its size remains smaller than, or comparable to, the SH that we find at all T studied here. Although there has been significant recent progress in identifying local structural properties (e.g. potential energy, soft vibrational modes) correlated to DH [6, 13, 14, 15], to our knowledge there are no reports of SH that exceeds the size of DH in the glass-forming regime, as we show here.

Our model system is the Kob-Andersen liquid, consisting of an 80:20 mixture of $N = 8788$ A and B particles, interacting via a potential $V_{\alpha\beta} = 4\epsilon_{\alpha\beta}[(\sigma_{\alpha\beta}/r)^{12} - (\sigma_{\alpha\beta}/r)^{6}]$ with $\alpha, \beta \in \{\mathrm{A}, \mathrm{B}\}$. All quantities are reported here in reduced units, with length, energy and time given relative to σ_{AA}, ϵ_{AA} and $(m\sigma_{AA}^2/48\epsilon_{AA})^{1/2}$ respectively, where m is the mass of the particles. The potential parameters are $\sigma_{AA} = 1.0$, $\epsilon_{AA} = 1.0$, $\sigma_{BB} = 0.88$, $\epsilon_{BB} = 0.5$, $\sigma_{AB} = 0.8$ and $\epsilon_{AB} = 1.5$ [7]. The potential is truncated and shifted at a cutoff radius of 2.5. All simulations are conducted in a cubic cell with periodic boundary conditions at a fixed volume V to give a density of 1.2. The simulation time step is $\Delta t = 0.01$. In all cases below, we restrict our attention to the properties of the A particles.

We study the liquid using the IC ensemble method at $T = 1.0$, 0.6, 0.5 and 0.466. At each T we generate 10 independent starting configurations. We first equilibrate a random configuration at $T = 5.0$ for at least 28 000 time steps, then reset T to the desired value, controlling T throughout with a Berendsen thermostat. Each system is equilibrated for at least $20\tau_\alpha$ where τ_α is the value of the α-relaxation time at that T. We then use each starting configuration to initiate $M = 500$ runs of an IC ensemble by randomizing the velocities of all particles according to a Maxwell-Boltzmann distribution, while leaving the particle coordinates unchanged. The IC ensemble runs are carried out in the microcanonical ensemble.

Let $r^2(i,k,t)$ be the squared displacement of the i-th A particle at time t in run k of an IC ensemble. The dynamic propensity of each A particle at time t is the value of $\langle r_i^2 \rangle_{\mathrm{ic}} = M^{-1} \sum_{k=1}^{M} r^2(i,k,t)$. We evaluate $\langle r_i^2 \rangle_{\mathrm{ic}}$ for each A particle as a function of t, and quantify the spatial correlations of this quantity, in terms of mobile and immobile domains, via a cluster analysis [14, 16]. We identify the particles having the highest 10% of $\langle r_i^2 \rangle_{\mathrm{ic}}$ values at a given t, and then find the clusters formed by this subset. Clusters are defined by the criterion that two particles of the subset that are also within $r = 1.4$ of one another (the position of the first minimum of the A-A radial distribution function) in the initial configuration are assigned to the same cluster. The number-averaged mean cluster size of a set of N_c clusters is

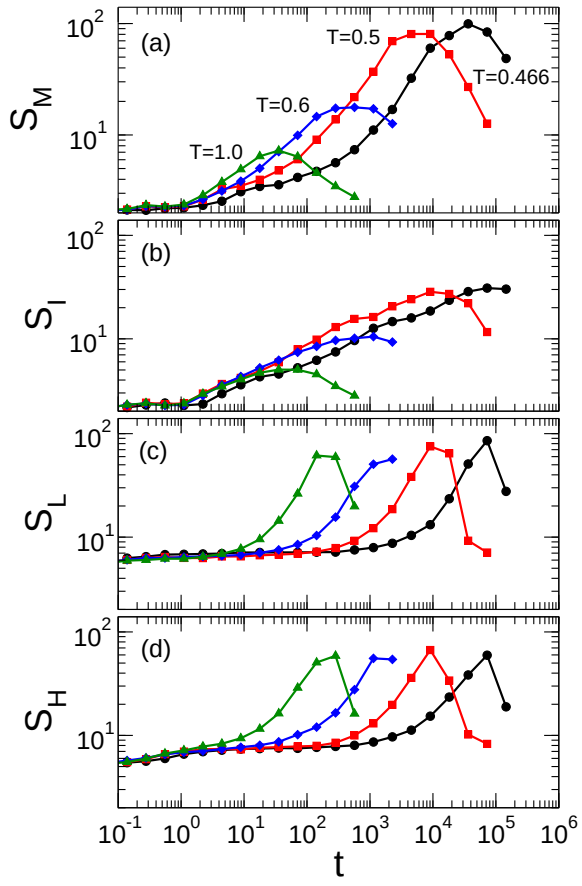

FIG. 1: Mean cluster size as a function of t for (a) mobile clusters, (b) immobile clusters, (c) clusters of A particles with low B coordination, and (d) clusters of A particles with high B coordination, all evaluated in the IC ensemble.

$S = (1/N_c)\sum_n nC(n)$, where $C(n)$ is the number of clusters of size n. We evaluate S for the clusters of mobile particles defined above, and denote it as S_M. We conduct the same analysis on the lowest 10% of $\langle r_i^2\rangle_{\rm ic}$ values, and find the mean cluster size of this immobile subset S_I. Figs. 1(a) and (b) show the t dependence of S_M and S_I, where the data are averaged over the 10 starting configurations used at each T.

For comparison, we also evaluate S for the DH that occurs in single simulation runs. That is, we separately analyze each of the $M = 500$ runs of one IC ensemble at each T, and evaluate, as a function of t, the mean cluster size S_m of the clusters formed by the particles having the largest 10% of displacements as measured from their position in the starting configuration. These mobile clusters correspond to the "strings" documented e.g. in Ref. [9]. We then obtain the average of the S_m curves over all 500 runs [Fig. 2(a)]. The corresponding cluster-size analysis of the smallest 10% of displacements in individual runs gives S_i as a function of t [Fig. 2(b)].

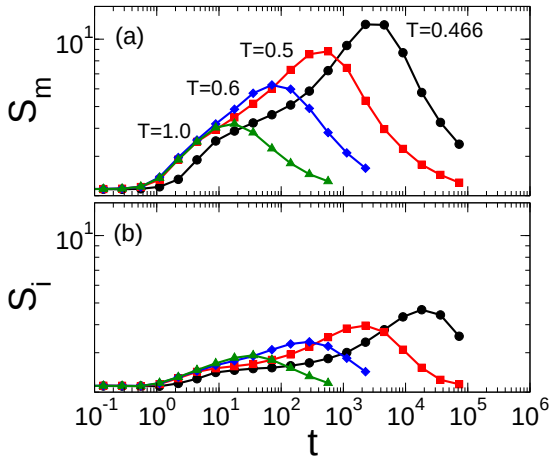

FIG. 2: Mean cluster size as a function of t for (a) mobile clusters and (b) immobile clusters, as measured in single simulations runs.

Fig. 1(a,b) and Fig. 2 allow us to compare the DH as revealed by both IC and conventional averaging, for both mobile and immobile domains. The t dependence of all curves follows the behavior for DH found in earlier work (see e.g. Ref. [16]). At small t, S has the value expected for a random choice of 10% of the A particles (approximately $S_o = 2.135$), consistent with no spatial correlations. However, on the time scale of structural relaxation a maximum occurs, indicating significant clustering of mobile and immobile particles. At large t, the DH begins to dissipate and S decreases toward S_o.

The monotonic increase in $S^{\rm max}$ (the maximum value of S) as T decreases quantifies the growth of DH on cooling. We denote the maximum value of S_M in Fig. 1(a) as $S_M^{\rm max}$; similarly, $S_I^{\rm max}$, $S_m^{\rm max}$ and $S_i^{\rm max}$ denote the maxima in Figs. 1(b), 2(a) and 2(b) respectively. The T dependence of $S^{\rm max}$ for all data in Figs. 1 and 2 is plotted in Fig. 3 as a function of $(T - T_c)/T_c$, where $T_c = 0.435$ is the critical temperature of mode coupling theory for the Kob-Andersen liquid. Fig. 3 shows that the sizes of the mobile and immobile clusters found using the IC ensemble are as much as an order of magnitude larger than the DH found when analyzing single runs. Also, the T dependence of $S^{\rm max}$ is quite different for the two kinds of averaging. $S_m^{\rm max}$ and $S_i^{\rm max}$ follow a power law [9, 17], while $S_M^{\rm max}$ and $S_I^{\rm max}$ do not. Indeed, the most notable behavior in Fig. 3 is that $S_M^{\rm max}$ and $S_I^{\rm max}$ both initially grow faster than a power law on cooling, but then at the lowest T their growth slows considerably.

To explore this behavior, in Fig. 4 (top panels) we visualize the mobile and immobile domains of the dynamic propensity for one starting configuration at each T, at the value of t corresponding to $S_M^{\rm max}$, where the clusters are most prominent [14]. Particles in the top (bottom) 50% of $\langle r_i^2\rangle_{\rm ic}$ values are represented as green (red) spheres, with each sphere plotted at the position of the particle in the initial configuration. The radius of each sphere

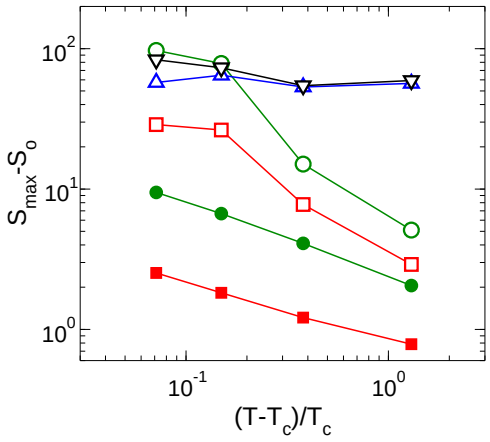

FIG. 3: Maximum value $S^{\max}$ of the mean cluster size for each of the curves plotted in Figs. 1 and 2, as a function of $(T-T_c)/T$, where $T_c = 0.435$. Shown are the maximum values of S_i (filled squares), S_m (filled circles), S_I (open squares), S_M (open cicles), S_H (up triangles) and S_L (down triangles). $S_o = 2.135$ has been subtracted from all the data to reflect the value of $S^{\max}$ in excess of its value for a random choice of 10% of the A particles. For the open symbols, the standard deviation of the data over the 10 starting configurations is less than or comparable to the symbol size.

represents the rank order of $\langle r_i^2 \rangle_{\rm ic}$: the larger a green (red) sphere is, the larger (smaller) is its value of $\langle r_i^2 \rangle_{\rm ic}$. (See caption of Fig. 4 for complete details.) These visualizations illustrate the increasing spatial correlation in the dynamic propensity as T decreases. At $T = 1.0$ the arrangement of red and green spheres is nearly random, while at the lowest T, very large mobile and immobile domains have emerged. At both $T = 0.5$ and 0.466, the domains are strikingly large, and are comparable to the system size. This suggests that finite-size effects may be responsible for the low T behavior of $S_M^{\max}$ and $S_I^{\max}$ in Fig. 3. We return to this issue below.

We next test for the presence of SH in the liquid, by analyzing a structural property of the system using the same IC averaging employed to find the dynamic propensity [14]. Specifically, we examine the chemical composition of the nearest neighbor environment of the A particles. Let $n(i,k,t)$ be the number of B particles found within a distance of $r = 1.2$ (the first minimum of the A-B radial distribution function) of the i-th A particle at time t in run k of an IC ensemble. We define the "B-coordination propensity" of each A particle at time t as $\langle n_i \rangle_{\rm ic} = M^{-1} \sum_{k=1}^{M} n(i,k,t)$. We show in Fig. 1(c) the time dependence of the mean cluster size S_L of the 10% of A particles with the lowest values of $\langle n_i \rangle_{\rm ic}$. Fig. 1(d) shows S_H, the mean cluster size of the 10% of A particles with the highest values of $\langle n_i \rangle_{\rm ic}$.

The time evolution of S_L and S_H in Fig. 1 is similar to S_M and S_I with one surprising exception: The values of $S_L^{\max}$ and $S_H^{\max}$ (shown in Fig. 3) are nearly independent of T, and are larger than or comparable to $S_M^{\max}$ and $S_L^{\max}$ for all T. The spatial variation of $\langle n_i \rangle_{\rm ic}$ is visualized in the bottom panels of Fig. 4 for the same initial configurations shown in the top panels, with t chosen at the time of $S_L^{\max}$. These visualizations confirm that the size of the domains with low and high B coordination remain large at all T, including at high T where the mobile and immobile domains are an order of magnitude smaller [18]. Further, the locations of the mobile and immobile domains that emerge on cooling approximately correspond with the domains of low and high B coordination that are prominent at all T. This spatial correspondence is consistent with expectation: an A particle with low B coordination will be less tightly bound by it's neighbors, and thus potentially more mobile, than one with high B coordination.

Hence, averaging a local structural property (here, the B coordination of A particles) in the IC ensemble reveals SH the size of which is insensitive to T over the range studied here. Of itself, this behavior is entirely consistent with the established view that structural correlation lengths do not grow significantly in most supercooled liquids. However, what is new in our results is that the observed SH is *larger* than or comparable to the DH by any of our measures (i.e. via IC or conventional averaging). In general, the increasing sensitivity of local dynamics to local structure as T decreases makes it inevitable that DH will occur in any liquid on a scale at least up to the size of any SH that is present. This scenario, in which DH is a dynamical consequence of an underlying SH, appears to apply in the range of T studied here.

We emphasize that since our main results are based on isoconfigurational averaging, the structural triggers for individual correlated dynamical events occurring in a single simulation run (e.g. the "strings" of Ref. [9]) are not specifically addressed here. Our results identify the structural properties that make such events more or less probable, and which induce the mobile and immobile domains visualized in Fig. 4.

An open question raised by our results is the role of finite size effects. The size of the domains observed in Fig. 4 certainly suggests that larger systems are required to fully understand the nature of the observed correlations, and their potential impact on other observables, both static and dynamic. For example, it is possible that in larger simulations the size of the DH may grow beyond that of the SH for $T < 0.5$. This would indicate an interesting crossover of the mechanism for DH, from one controlled by SH, to one allowing growth beyond the scale set by SH. However, our conclusions as they apply to DH for $T > 0.5$ are unlikely to change in simulations of larger systems, since the DH becomes smaller than the system size in this regime.

We thank ACEnet for providing computational resources, and NSERC, CFI and AIF for financial support. GSM is supported by an ACEnet Research Fellowship, and PHP by the CRC program.

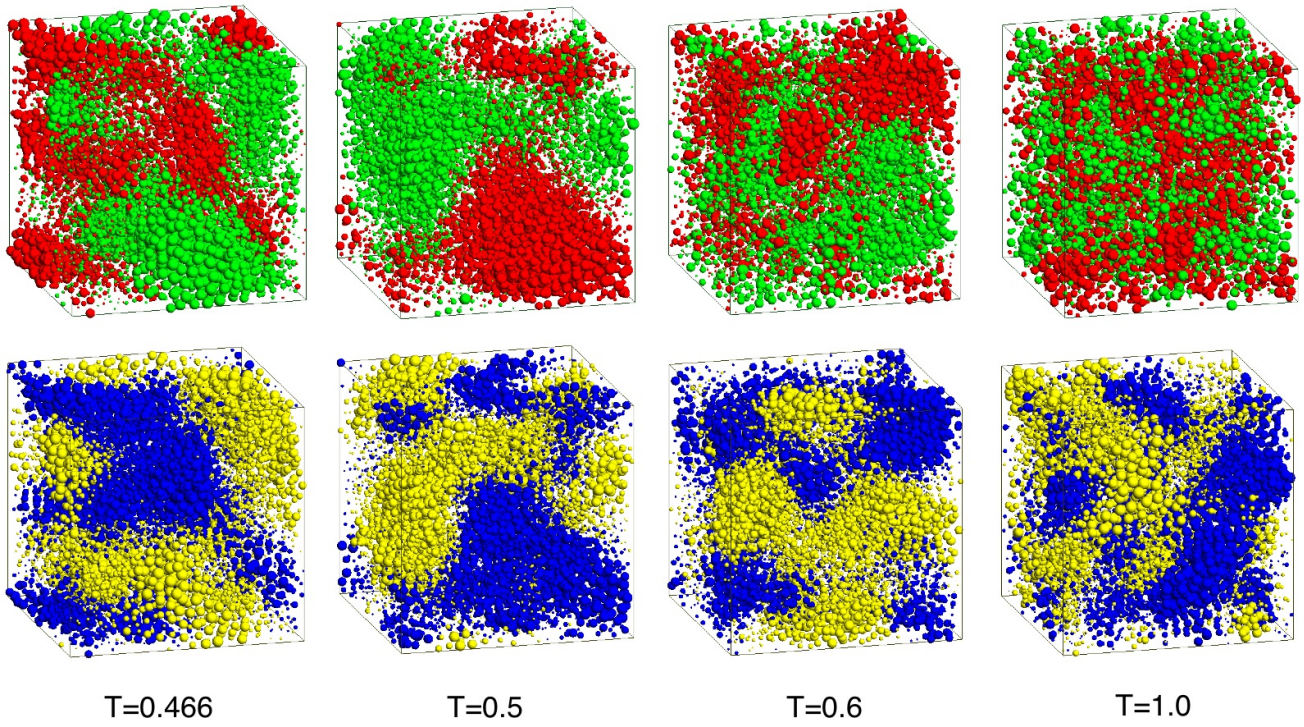

FIG. 4: Spatial variation of $\langle r_i^2 \rangle_{\rm ic}$ (top panels) and $\langle n_i \rangle_{\rm ic}$ (bottom panels) at each T. To make each top panel, the values of $\langle r_i^2 \rangle_{\rm ic}$, evaluated at the time of the maximum of S_M, are assigned to each A particle at its position in the initial configuration of the IC ensemble. These values are sorted and assigned an integer rank R_i from 1 to N, from smallest to largest. Each A particle is then plotted as a green sphere of radius $\sigma = R_{\rm min} \exp\{[(R_i - N)/(1 - N)] \log(R_{\rm max}/R_{\rm min})\}$, where $R_{\rm max} = 0.5$ and $R_{\rm min} = 0.01$. The ranks R_i are then reversed (i.e. assigned from largest to smallest), and each A particle is also plotted as a red sphere of radius σ. The color observed for each particle therefore indicates which of the green or red spheres is larger. The result presents the rank of $\langle r_i^2 \rangle_{\rm ic}$ on an exponential scale, such that the largest green spheres represent the most mobile A particles, and the largest red spheres the most immobile. The bottom panels are created in exactly the same way as the top panels, but with $\langle r_i^2 \rangle_{\rm ic}$ replaced by $\langle n_i \rangle_{\rm ic}$, and where the time is chosen to be the maximum of S_L at each T. In the bottom panels, the largest yellow spheres represent the A particles with the lowest B coordination, and the largest blue spheres the A particles with the highest B coordination.

[1] P.G. Debenedetti, *Metastable Liquids. Concepts and Principles* (Princeton University Press, Princeton, New Jersey, 1996).

[2] P.G. Debenedetti and F.H. Stillinger, Nature **410**, 259 (2001).

[3] H.C. Andersen, Proc. Natl. Acad. Sci. U.S.A. **102**, 6686 (2005).

[4] A. Widmer-Cooper, P. Harrowell and H. Fynewever, Phys. Rev. Lett. **93**, 135701 (2004).

[5] A. Widmer-Cooper and P. Harrowell, Phys. Rev. Lett. **96**, 185701 (2006).

[6] A. Widmer-Cooper, H. Perry, P. Harrowell and D.R. Reichman, Nature Physics **4**, 711 (2008).

[7] W. Kob and H.C. Andersen, Phys. Rev. E **51**, 4626 (1995); Phys. Rev. E **52**, 4134 (1995).

[8] S. Sastry, P.G. Debenedetti and F.H. Stillinger, Nature **393**, 554 (1998).

[9] C. Donati, S.C. Glotzer, P.H. Poole, W. Kob and S.J. Plimpton, Phys. Rev. E **60**, 3107 (1999).

[10] G. A. Appignanesi, J. A. Rodriguez Fris, R. A. Montani, and W. Kob, Phys. Rev. Lett. **96**, 057801 (2006).

[11] L. Berthier and R.L. Jack, Phys. Rev. E **76**, 041509 (2007).

[12] R.S.L. Stein and H.C. Andersen, Phys. Rev. Lett. **101**, 267802 (2008).

[13] L.A. Fernández, V. Martín-Mayor and P. Verrocchio, Phys. Rev. E **73**, 020501 (2006).

[14] G.S. Matharoo, M.S.G. Razul and P.H. Poole, Phys. Rev. E **74**, 050502(R) (2006).

[15] P. Chaudhuri, S. Sastry and W. Kob, Phys. Rev. Lett. **101**, 190601 (2008).

[16] M. Vogel and S.C. Glotzer, Phys. Rev. Lett. **92**, 255901 (2004); Phys. Rev. E **70**, 061504 (2004).

[17] While power law growth of the size of mobile clusters in single runs is well known, our results show that the immobile clusters also exhibit a power law growth with approximately the same exponent as for mobile clusters.

[18] We also note that instantaneous spatial correlations of particles with low and high B coordination exist in the system. This can be seen from the fact that the small t limit of the curves in Figs. 1(c) and (d) have a value larger than S_o.